SSRG International Journal of Civil Engineering
ISSN: 2348-8352/ https://doi.org/10.14445/23488352/IJCE-V13I9P117

Volume 13 Issue 9, 284-301, September 2026

Original Article

Performance Assessment of High Strength Self-Compacting Concrete Beams with Web Reinforcement

Anitha J[1*], Ravi Kumar H.[1], Tamil Selvi N.[1], K. V. R. Prasad[1], Subramanya K. G.[2]

[1]*Department of Civil Engineering, Sir M Visvesvaraya Institute of Technology, Bengaluru, India.*
[2]*Department of Civil Engineering, Government Engineering College, Kushalnagar, India.*

[1]*Corresponding Author : anitha_civil@sirmvit.edu*

Received: 02 June 2026 Revised: 02 September 2026 Accepted: 05 September 2026 Published: 29 September 2026

Abstract - *Self-Compacting Concrete (SCC) is a highly flowable material that achieves full compaction without external vibration, making it particularly suitable for heavily reinforced structural members where conventional compaction is difficult. Since shear failure is typically sudden and brittle, understanding the shear response of SCC members is essential for ensuring structural safety. Although extensive research has been conducted on SCC, the shear behaviour of high-strength SCC produced with manufactured sand remains insufficiently explored. The novelty of this study lies in the experimental investigation of the shear performance of M70-grade SCC incorporating manufactured sand and the evaluation of its behaviour against multiple design models and analytical approaches. Six reinforced concrete beams are cast with a constant longitudinal reinforcement ratio (ρt) and varying shear reinforcement ratios (ρs). Experimental observations include cracking load, ultimate load, crack width, midspan deflection, and one-third span deflection. The obtained results are analysed using codal provisions, established shear strength equations, and numerical predictions from Response 2000 software. The experimental results show that flexural cracks develop initially, followed by shear cracks within the shear span as loading increases. Beams failing in flexure exhibit widening tension cracks and compression-zone spalling, whereas beams failing in shear display rapid propagation of diagonal cracks toward the supports and loading points, resulting in brittle failure. Comparisons between experimental and predicted shear strengths indicate that most analytical models underestimate the measured capacity. Among the evaluated approaches, AS 3600 provides the closest agreement with experimental results, yielding a mean prediction ratio of 0.783 and a coefficient of variation of 23.72%.*

Keywords - *Concrete beams, Manufactured sand, Self-compacting concrete, Shear behavior, Web-reinforcement.*

1. Introduction

The use of Self-Compacting Concrete (SCC) has provided an effective solution for concreting structural members in which conventional vibration is difficult because of closely spaced reinforcement or restricted access. Unlike conventionally placed concrete, SCC is designed to flow under its own weight, pass through reinforcement without blockage and occupy the formwork without mechanical compaction. These characteristics can improve the quality of concrete placement while reducing the dependence on labour-intensive vibration. The required combination of filling ability, passing ability and resistance to segregation is primarily controlled by the proportions and interaction of cementitious materials, fine aggregate, water and superplasticizer. Consequently, the selection and characteristics of fine aggregate have an important role in determining the fresh and hardened performance of SCC.

The increasing demand for natural river sand has raised concerns regarding its availability and the environmental consequences associated with excessive extraction. Manufactured sand (M-sand), obtained by crushing and processing hard rock such as granite or basalt, is therefore being increasingly considered as an alternative fine aggregate. Unlike naturally occurring river sand, M-sand can be produced with controlled particle size distribution through successive crushing and screening operations. Its particle angularity, surface texture and grading characteristics can influence particle packing, paste demand and the overall behaviour of concrete. These characteristics become particularly relevant in SCC, where the balance between flowability and stability is essential. The use of M-sand in High-Strength Self-Compacting Concrete (HSSCC) can therefore provide both a structural and environmental advantage; however, its influence should also be assessed at the structural-member level rather than being limited to material properties.

Among the different structural responses that require attention, the shear behaviour of reinforced concrete beams is particularly important. Shear failure is generally sudden and brittle, leaving considerably less warning than flexural failure. The resistance of a reinforced concrete beam to shear does not depend on a single material or geometric parameter. It results from the combined action of several mechanisms, including the tensile contribution of concrete, aggregate interlock, dowel action of longitudinal reinforcement, contribution of transverse reinforcement, bond between concrete and reinforcement, and the geometry of the beam. The relative contribution of these mechanisms can change with concrete strength, reinforcement ratio, shear span-to-effective-depth ratio (a/d), aggregate characteristics and beam size. These interactions make the prediction of shear capacity considerably more complex than that of flexural capacity.

The difficulty is further increased when high-strength concrete is combined with self-compacting characteristics. An increase in compressive strength does not necessarily produce a proportional increase in shear resistance, and high-strength concrete may exhibit comparatively brittle behaviour after cracking. At the same time, the aggregate characteristics of M-sand can influence crack development and aggregate interlock, which are important components of shear resistance. Hence, the shear response of HSSCC containing M-sand cannot necessarily be inferred directly from the established behaviour of conventional reinforced concrete beams. Experimental investigation is therefore necessary to establish the structural response of such members and to examine whether existing shear-strength formulations remain appropriate.

Considerable research has been undertaken to understand the parameters governing the shear strength of reinforced concrete beams. Kani [10], Rajagopalan and Ferguson [11], and Zsutty [5] related the shear capacity of singly reinforced beams to concrete compressive strength. However, the experimental evidence reported by several researchers has indicated that the relationship between concrete strength and shear resistance is not adequately represented by a simple strength-based relationship. The ACI 318 provisions [12], for example, express the concrete contribution to shear resistance in terms of the square root of the characteristic compressive strength, $\sqrt{f'c}$. Zsutty [5] and Diaz de Cassio et al. [13] reported that the effects of longitudinal reinforcement ratio and a/d ratio were not adequately represented in the ACI approach. Mathey and Watstein [14] examined the influence of concrete tensile strength and a/d ratio and reported that the tensile properties of longitudinal reinforcement did not significantly affect the shear failure load of the beams investigated.

The role of reinforcement arrangement and beam geometry has also been examined in several investigations. Boris and Scordelis [15] investigated beams with different transverse reinforcement arrangements and a/d ratios and reported an increase in shear resistance when multilayer longitudinal tensile reinforcement was used. Krefeld and Thurston [16] examined the influence of compressive strength, steel ratio, span and loading conditions in members with and without transverse reinforcement and demonstrated that additional resistance could develop beyond the nominal shear-failure level depending on the a/d ratio. Zsutty [17] further reported that support and loading conditions influenced the shear response of reinforced concrete beams, although the proposed equation did not explicitly incorporate these parameters. Mattock et al. [18] investigated reinforced concrete beams subjected to axial forces and observed that the provisions of ACI Committee 318 [19] and ACI-ASCE 426 [20] could underestimate the shear capacity of members subjected to axial loading.

Beam dimensions and aggregate-related parameters constitute another important group of variables affecting shear resistance. Bazant et al. [21] demonstrated the significance of beam size and developed empirical relationships that produced lower variability than several earlier approaches. Bazant and Sun [22] subsequently incorporated aggregate size and transverse reinforcement into a model for predicting shear failure. Bentz [33] also proposed an expression for shear capacity that considers aggregate size, longitudinal tensile reinforcement and beam geometry. These investigations collectively indicate that shear resistance is controlled by the interaction of material, reinforcement and geometric parameters rather than by concrete compressive strength alone.

The applicability of established design provisions to high-strength and shear-critical beams has also been questioned. Roller and Russell [23] investigated high-strength shear-critical beams with web reinforcement and reported that the ACI Committee 318 provisions [12] could overestimate the shear capacity. Kim et al. [24] similarly observed limitations in the ACI approach for larger beams and reported comparatively better predictions using the CEB-FIP Model Code [25]. Their findings also indicated that beam size affects the shear strength of both normal-strength and high-strength concrete beams. Ahmad et al. [26] observed a reduction in ductility with increasing concrete compressive strength in shear-critical beams. Watanabe and Lee [27] developed a truss-mechanism-based approach for predicting failure mode and ultimate strength and reported satisfactory agreement with previously available results. Yoon, Cook and Mitchell [28] examined the minimum shear reinforcement requirements for different concrete strength levels and reported that the CSA provisions [29] provided an adequate reserve of strength compared with the ACI criteria.

Further work has attempted to improve the prediction of shear capacity through modified analytical and empirical approaches. Angelakos et al. [30] reported that weakly reinforced, shear-controlled beams may not possess adequate safety margins under existing provisions and questioned the adequacy of the ACI 318 [1] approach for contemporary concrete construction. Cladera and Mari [31] performed a detailed investigation of shear strength and developed an Artificial Neural Network (ANN) approach for predicting beam shear capacity together with alternative design expressions. Cladera and Mari [32] proposed a variable-angle truss-based procedure incorporating concepts from modified compression field theory for beams provided with stirrups. Lee et al. [34] examined beams containing high-strength transverse reinforcement and observed an inverse relationship between crack width and the ratio of transverse steel strength to concrete strength. Mansour and Tayeh [35] proposed shear-strength equations for normal and fibre-reinforced concrete beams while accounting for the a/d ratio and highlighted limitations in the treatment of this parameter in EC2 and ACI provisions. Söğüt [36] reported that an increase in the longitudinal tension reinforcement ratio enhanced shear capacity, while concrete compressive strength and beam size also had significant effects on shear stress and capacity.

The development of the ACI provisions reflects the continuing difficulty in obtaining a generally applicable expression for shear resistance. ACI 318 [1] introduced an equation for evaluating the shear strength of beam sections without web reinforcement. Subsequent experimental studies, however, indicated limitations in the ACI 318-14 formulation [2], particularly for larger beams having minimum reinforcement and no shear reinforcement. A revised one-way shear design expression was subsequently incorporated in ACI 318-19 [3]. Earlier investigations [4-9] also identified limitations associated with beam size, arch action and other mechanisms contributing to shear resistance. Since several established design relationships were developed largely from experimental databases involving conventional concrete, their suitability for high-strength self-compacting concrete containing manufactured sand requires specific examination.

1.1. Research Gap and Objective of the Present Study

The preceding studies demonstrate that the shear response of reinforced concrete beams is influenced by concrete strength, beam size, a/d ratio, longitudinal and transverse reinforcement, aggregate characteristics and loading conditions. Nevertheless, the available research does not provide sufficient experimental evidence on the combined behaviour of high-strength self-compacting concrete beams incorporating manufactured sand and transverse reinforcement. Much of the established shear research has been based on conventional vibrated concrete, while investigations dealing with SCC have more commonly concentrated on its fresh, mechanical or durability characteristics rather than the shear response of structural members. Consequently, the applicability of existing shear-strength relationships to HSSCC containing M-sand remains insufficiently established.

A further issue concerns the interaction between the material characteristics of HSSCC and the mechanisms responsible for shear transfer. The use of manufactured sand changes the aggregate characteristics of the concrete, while the high-strength matrix and self-compacting nature of the concrete can influence cracking, aggregate interlock and the interaction between concrete and reinforcement. The resulting shear response may therefore differ from that represented by empirical relationships developed using conventional concrete. In addition, the influence of transverse reinforcement on the shear response of M-sand-based HSSCC beams and the ability of existing design equations to reproduce the experimentally observed capacity require further assessment.

Accordingly, the present investigation focuses on the experimental assessment of the shear behaviour of reinforced HSSCC beams produced using manufactured sand as fine aggregate. Six reinforced concrete beams having dimensions of 125 × 250 × 2000 mm were cast, cured and tested under a loading frame. The specimen dimensions were selected considering the available testing facility and an appropriate span-to-effective-depth ratio so that the specimens did not fall within the deep-beam category. The experimental programme incorporates continuous longitudinal reinforcement and different levels of transverse reinforcement to examine their influence on the shear response of the HSSCC beams. The investigation considers the observed cracking behaviour, failure mode and ultimate load of the tested beams. The experimentally obtained shear capacities are subsequently examined against selected analytical and codal predictions to assess the applicability of existing shear-strength approaches to the investigated HSSCC system. The principal contribution of the study is therefore the experimental characterization and analytical assessment of the shear response of M-sand-based HSSCC beams with transverse reinforcement, an area for which comparatively limited structural-level evidence is available. The results provide a basis for assessing the adequacy of existing shear-strength provisions and for identifying the parameters that require consideration when evaluating HSSCC beams containing manufactured sand.

1.2. Recent Developments in Shear Reinforcement of HSSCC and SCC Beams

Recent research on the shear behaviour of self-compacting and high-strength concrete beams has considered both conventional transverse reinforcement and alternative or supplementary shear-resisting systems. Conventional stirrups continue to be an important parameter in HSSCC beams because the shear response is governed by the interaction of concrete strength, aggregate characteristics, beam geometry and reinforcement. Zende et al. [39] experimentally investigated HSSCC slender beams with different concrete strengths and stirrup spacings. Their study examined the influence of varying stirrup spacing on the shear behaviour of HSSCC and also assessed the applicability of different design provisions. The findings confirmed the importance of transverse reinforcement in the shear response of HSSCC beams and highlighted the need for careful assessment of code-based shear predictions for high-strength self-compacting concrete.

The use of steel fibres has also been investigated as an alternative or supplementary mechanism for resisting shear. Sagi et al. [40] experimentally studied self-compacting concrete deep beams containing macro steel fibres at different volume fractions and compared their behaviour with beams incorporating web reinforcement. The study showed that steel fibres enhanced the shear response and that an appropriate fibre content could provide a contribution comparable with a specified level of web reinforcement. However, the investigation was conducted on deep beams with a low shear-span-to-depth ratio, and therefore, its findings cannot be directly transferred to slender HSSCC beams. Savaris and Laufer [41] evaluated the shear strength of steel-fibre self-compacting concrete beams using a database of 113 experimental results. Their assessment showed that increasing fibre volume generally increased shear strength within the range investigated and also demonstrated differences between the performance of code-based and empirical shear-strength equations for fibre-reinforced SCC.

Hybrid fibre systems have subsequently been considered to combine the different crack-control mechanisms provided by steel and synthetic fibres. Alkhattat and Al-Ramahee [42] experimentally investigated lightweight self-compacting concrete beams incorporating steel fibres and hybrid steel–polypropylene fibres. The study reported changes in shear performance associated with fibre incorporation, although the concrete system involved lightweight aggregate and therefore differs from the normal-weight HSSCC considered in the present investigation. Silva et al. [43] further examined self-compacting concrete beams without stirrups containing steel and synthetic fibres. Both steel-fibre and hybrid-fibre mixtures provided higher shear strength before shear cracking than the reference concrete, while the principal benefit of fibre incorporation was observed in the residual post-cracking response. These findings demonstrate the potential of distributed fibres to contribute to shear resistance, but they also represent a different reinforcement mechanism from conventional transverse reinforcement.

Research on high-strength concrete has also examined the combined use of different fibre types and conventional reinforcement. Awad et al. [44] investigated high-strength concrete beams incorporating hybrid steel and polypropylene fibres and considered the effects of parameters including transverse reinforcement and shear-span-to-depth ratio. The study combined experimental investigation with numerical modelling and comparison with ACI provisions. Such work indicates that the contribution of distributed fibres is influenced by their interaction with the existing reinforcement and beam geometry rather than acting as an independent replacement for conventional shear reinforcement in all cases.

Alternative reinforcement materials have also been examined in self-compacting concrete members. Abbas et al. [45] investigated high-strength self-compacting concrete deep beams reinforced using combinations of steel and GFRP bars and considered different steel-fibre contents. Their results showed that steel fibres increased the shear capacity of the investigated deep beams, while the study also examined the contribution of GFRP reinforcement to shear resistance through dowel action.

The authors reported that the dowel contribution associated with GFRP bars was comparable with that of steel bars having the same reinforcement area. However, the specimens were deep beams and incorporated hybrid longitudinal reinforcement, making the configuration different from the slender beams considered in the present study.

More recent work has explored combinations of fibre reinforcement and prestressing as a shear-strengthening strategy. Choi et al. [46] investigated self-compacting lightweight concrete beams incorporating steel fibres and unbonded prestressing bars, while varying prestressing force and transverse reinforcement ratio. Steel fibres substantially increased the normalized shear capacity, and the combined use of fibres and prestressing changed the observed failure mode from shear to flexure in the investigated specimens. The study demonstrates the potential of combining different shear-resisting mechanisms, although the use of lightweight aggregate and prestressing distinguishes the specimens from the M-sand-based HSSCC beams investigated herein.

The recent literature therefore demonstrates that shear resistance in SCC and HSSCC members can be enhanced through conventional stirrups, distributed fibres, hybrid fibre systems, FRP reinforcement and combinations of reinforcement mechanisms. Nevertheless, these studies differ considerably in concrete composition, aggregate type, beam geometry, reinforcement arrangement and loading configuration. In particular, studies on HSSCC with conventional transverse reinforcement have not generally addressed the combined influence of manufactured sand and transverse reinforcement in slender beams.

The present study is therefore positioned within this research area by experimentally investigating the shear behaviour of HSSCC beams produced using manufactured sand as fine aggregate and provided with transverse reinforcement. The study further evaluates the experimentally obtained shear response against selected analytical and codal approaches. The contribution of the present investigation is consequently not the introduction of a new type of shear reinforcement, but the structural-level assessment of M-sand-based HSSCC with transverse reinforcement and the evaluation of existing shear-strength approaches for this particular material and reinforcement combination.

2. Materials and Experimental Methodology

2.1. Materials

A High-Strength Self-Compacting Concrete (HSSCC) of nominal grade M70 was used for the fabrication of all beam specimens. Birla Super Cement of 53 grade conforming to IS 269:2015 was used as the principal cementitious material. The specific gravity of the cement was 3.07. Class-F fly ash obtained from Raichur Thermal Power Plant was incorporated as a supplementary cementitious material, replacing 20% of the cement, and had a specific gravity of 2.40.

Air-Classified Manufactured Sand (AGMS) was used as the fine aggregate in all the concrete mixtures. The specific gravity of the manufactured sand was 2.56. Crushed granite was used as coarse aggregate. The coarse aggregate had a specific gravity of 2.65 and a nominal size within the range of 4.75–12.5 mm. The use of manufactured sand was maintained throughout the experimental programme so that the influence of the transverse reinforcement could be examined without introducing variation in the type of fine aggregate.

Potable water free from harmful impurities and salts was used for mixing and curing, while maintaining a water binder ratio of 0.33. Master Glenium SKY 8233, a carboxylic-ether-polymer-based superplasticizer, was used to obtain the flowability required for self-compacting concrete. The relative density of the superplasticizer was 1.09 ± 0.01, and the product complies with IS 9103:2003 and ASTM C494 Types A and F. Glenium Stream-2 was used as a chloride-free viscosity-modifying agent to improve the stability of the concrete mixture.

The mix proportions adopted for the M70 HSSCC are presented in Table 1. Maintaining a common concrete mixture for all beam specimens ensured that the principal material characteristics remained constant while the transverse reinforcement parameters were varied.

Table 1. The summarized mix proportioning of HSSCC - M70

Ingredient	CA	FA	Cement	Fly ash	Water	Super Plasticizer	VMA
Quantity (kg/m^3)	768.88	834.40	400.00	142.64	179.35	9.22	1.08

2.2. Fresh Properties of SCC

Table 2 represents the fresh value properties of M70 HSSCC used in this study. It was observed that the mix satisfied the flow property requirements as recommended by EFNARC.

Table 2. Values for fresh property tests

Test	Expt. Value	EFNARC Range
Slump Flow Diameter	740	650 – 800 mm
T500 Time	2.6	2 – 5 seconds
V-Funnel Time	6.5	6 – 12 seconds
L-Box (H2/H1 Ratio)	0.95	≥ 0.8 (preferably ≥ 0.9)

2.3. Experimental Programme and Specimen Design

The experimental programme comprised six reinforced concrete beams cast using the same M70 HSSCC mixture. The principal experimental variable was the transverse reinforcement, which was varied in terms of stirrup diameter and spacing. The longitudinal reinforcement was kept constant for all specimens. This arrangement was adopted to isolate the influence of transverse reinforcement on the shear response of the beams.

Each beam had a rectangular cross-section of 125 mm × 250 mm, a total length of 2000 mm and an effective span of 1800 mm. The selected dimensions were governed by the available loading facility and by the requirement to obtain a beam configuration representative of a slender member rather than a deep beam. The specimens, therefore, provided an appropriate configuration for examining the development of diagonal shear cracking and the contribution of transverse reinforcement to shear resistance.

Six reinforcement configurations were investigated. Beams AC1, AC2 and AC3 contained 6 mm diameter stirrups at spacings of 250, 200 and 150 mm, respectively. Beams AC4, AC5 and AC6 contained 8 mm diameter stirrups at spacings of 200, 150 and 100 mm, respectively. The longitudinal reinforcement ratio was maintained at 2.413% for all six beams. The corresponding shear reinforcement ratios ranged from 0.181% to 0.805%.

The experimental matrix is summarized in Table 3. The measured concrete compressive strengths at the time of beam testing ranged from 68.43 to 74.86 MPa, confirming the high-strength nature of the concrete used in the experimental programme.

Table 3. Beam dimensions with specifications

Beam Designation	ρ (%)	f_{ck}	$ρ_w$ (%)	Shear Spacing (2L @ c/c)
AC1/6ϕ250	2.413	72.19	0.18103	6ϕ@250
AC2/6ϕ200	2.413	73.77	0.22629	6ϕ@200
AC3/6ϕ150	2.413	68.43	0.30171	6ϕ@150
AC4/8ϕ200	2.413	71.38	0.40229	8ϕ@200
AC5/8ϕ150	2.413	72.78	0.53638	8ϕ@150
AC6/8ϕ100	2.413	74.86	0.80457	8ϕ@100

2.4. Rationale for Selection of Experimental Variables

The experimental programme was designed to examine the effect of transverse reinforcement while minimizing the influence of other variables. Accordingly, the concrete mixture, beam cross-section, span, longitudinal reinforcement ratio and curing period were kept constant. Variation was introduced through two parameters of the transverse reinforcement: bar diameter and spacing.

The selected combinations provided a progressive increase in the shear reinforcement ratio. For the 6 mm stirrups, reducing the spacing from 250 to 150 mm increased the reinforcement ratio from 0.181% to 0.302%. For the 8 mm stirrups, the spacing was varied from 200 to 100 mm, resulting in reinforcement ratios between 0.402% and 0.805%. This arrangement permitted examination of the response over a range of transverse reinforcement levels rather than relying on a single reinforcement configuration.

The use of six specimens was therefore associated with the two-reinforcement series adopted in the experimental programme: three specimens with 6 mm stirrups and three specimens with 8 mm stirrups. The resulting matrix allowed the effects of both stirrup diameter and spacing to be examined within the available experimental facility while keeping the principal material and geometric parameters unchanged.
It should be noted that the experimental programme was not designed as a large statistical population study. The six specimens were selected to provide a controlled experimental comparison of the specified reinforcement configurations. Consequently, the statistical interpretation of the results is restricted to the observed experimental trends and relationships within the investigated range.

2.5. Beam Fabrication and Curing

The six-beam specimens were cast using the M70 HSSCC mixture described in Section 2.1. The reinforcement cages were prepared according to the respective configurations listed in Table 3, with continuous longitudinal reinforcement and stirrups provided throughout the beam length.

Following casting, the specimens were cured for 28 days under normal temperature. Also, the companion strength specimens were cured under the same curing conditions for a period of 28 days before testing. After completion of curing, the external surfaces of the beams were whitewashed to provide a contrasting background for visual identification and measurement of cracks during loading. This preparation facilitated the observation of crack initiation, propagation and changes in crack width throughout the test.

2.6. Test Setup and Loading Procedure

After 28 days of curing, each beam was positioned in the loading frame with the supports and loading arrangement corresponding to the experimental configuration. The beam was instrumented to measure the applied load and vertical deflection at selected locations. Deflection measurements were obtained at the midspan and at the one-third-span locations.

The beams were loaded incrementally using a hydraulic jack. The load was increased in increments of 4 kN, and the corresponding deflection readings were recorded at each loading stage. The load corresponding to the first visible crack was identified and recorded as the cracking load (P_{cr}). Crack development was monitored throughout the test, and crack widths were measured using a handheld microscope.

Loading was continued beyond crack initiation until the specimen reached its ultimate load and subsequently failed. The ultimate load, crack development, deflection response and final failure mode were recorded for each specimen. This procedure enabled the relationship between applied load, deformation, cracking and ultimate shear response to be established for each reinforcement configuration.

2.7. Instrumentation and Measurements

The experimental measurements comprised applied load, vertical deflection and crack width. Deflection was monitored at the midspan and one-third-span locations, allowing both the overall deformation response and the development of the deflected beam profile to be assessed. Crack widths were measured at the critical stages of loading using a handheld microscope.

The applied load was monitored through the proving-ring/loading arrangement associated with the hydraulic loading system. The manuscript records the load at every 4 kN increment, while the corresponding deflection measurements were recorded at the specified gauge locations. The same measurement procedure was followed for all six specimens to maintain consistency between tests.

The present manuscript does not contain the manufacturer's accuracy, least count or formal calibration records for the load and displacement measuring devices. Accordingly, no numerical measurement uncertainty has been introduced into the present analysis. These details should be added if the original laboratory test records contain the relevant calibration certificates or instrument specifications.

2.8. Recorded Response Parameters

The experimental observations were organized around four principal response parameters: cracking load, crack width, deflection and ultimate load. The cracking load was used to identify the onset of visible cracking, while crack-width measurements provided an indication of crack development with increasing load. Load–deflection data obtained at the midspan and one-third-span locations were used to assess the deformation response of the specimens.

The ultimate load was taken as the maximum load sustained by the beam before failure. The observed crack pattern and final failure mode were also recorded. These measurements formed the basis for subsequent comparison of the six beam configurations and for evaluating their shear capacities against the selected codal and analytical approaches.

3. Results and Discussions

The data recorded during the testing of beams were analysed and the crack propagation and the failure mode were studied in detail. Tables and figures illustrating the results have been given and discussed in the following sections.

3.1. Load vs Deflection Pattern

The load-deflection responses of the six HSSCC beams are presented in Figure 1. The experimental results demonstrate a distinct change in structural response after cracking, followed by nonlinear deformation until the ultimate load was reached. The beams exhibited an approximately linear response during the initial stage of loading, indicating predominantly elastic behaviour before significant cracking. With further increase in load, the development and propagation of flexural and shear cracks resulted in a progressively nonlinear response.

Beam AC1 (6ϕ250) attained an experimental ultimate load of approximately 225 kN, corresponding to an ultimate shear force of 116 kN. Increasing the transverse reinforcement by reducing the stirrup spacing from 250 to 200 mm in AC2 (6ϕ200) increased the ultimate load to approximately 235 kN, while AC3 (6ϕ150) attained approximately 275 kN. The corresponding experimental shear forces were 120 and 169 kN, respectively. Thus, within the 6 mm stirrup series, reducing the spacing from 250 to 150 mm increased the measured shear capacity by approximately 45.7%.

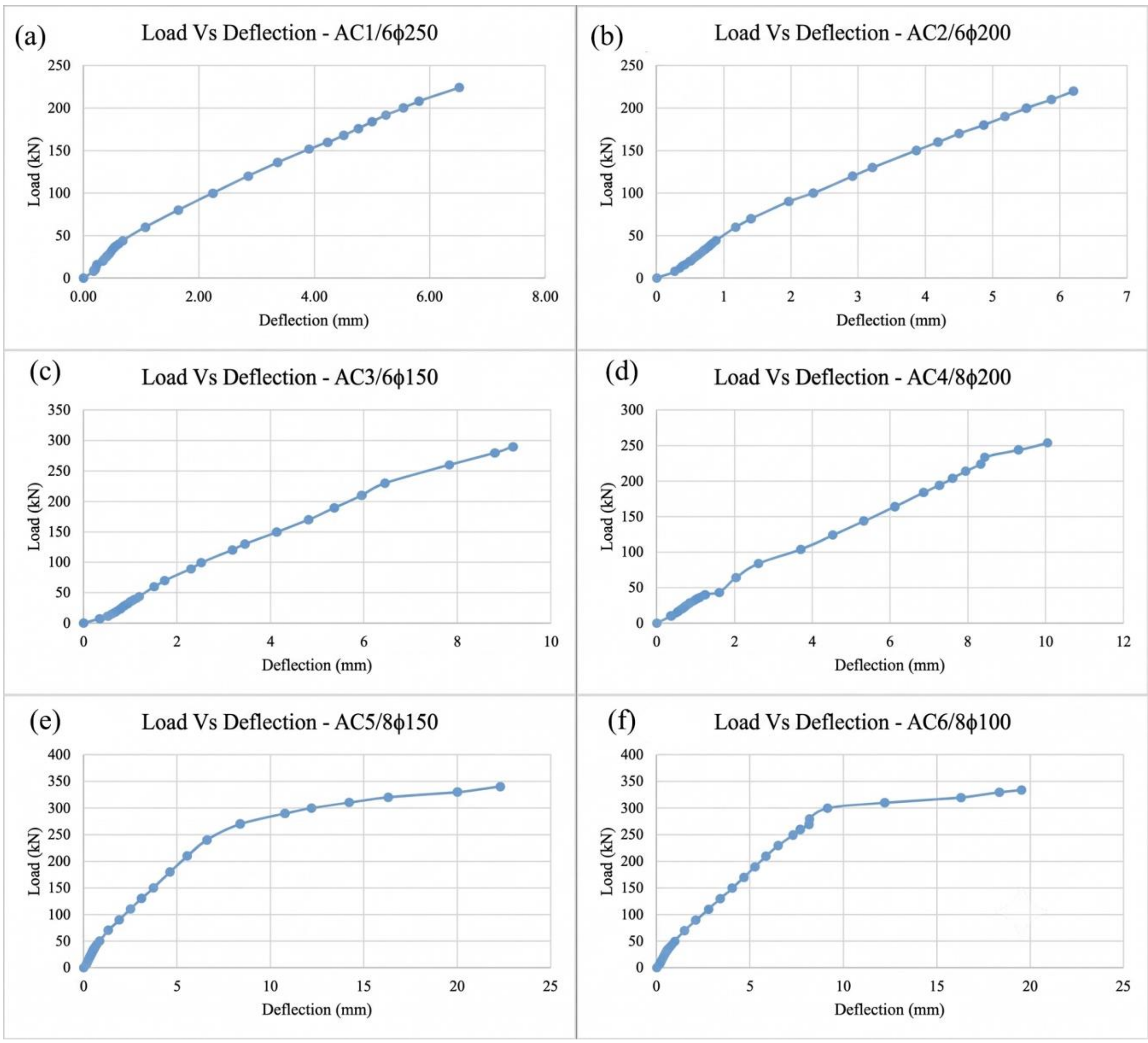

Fig. 1 Load vs deflection plot for HSSCC beams AC1-AC6

A similar trend was observed for the beams containing 8 mm diameter stirrups. AC4 (8ϕ200), AC5 (8ϕ150) and AC6 (8ϕ100) developed experimental shear forces of 154, 170 and 170 kN, respectively. The corresponding load–deflection curves show that the beams with the denser transverse reinforcement generally sustained greater deformation before reaching their ultimate response. The increase in capacity was more pronounced when the 8 mm stirrups were introduced at the higher reinforcement levels. However, the similar ultimate shear forces of AC5 and AC6 indicate that increasing the transverse reinforcement beyond the AC5 configuration did not result in a proportional increase in the measured ultimate shear force.

The observed behaviour indicates that transverse reinforcement contributes to shear resistance by restraining the development and widening of diagonal cracks and by providing additional tensile resistance across the shear cracks. Nevertheless, the results also indicate that the increase in shear capacity is not necessarily proportional to the increase in transverse reinforcement. This observation is important when interpreting the influence of reinforcement ratio because both stirrup diameter and spacing were varied in the present experimental programme.

The deformation response also indicates improved post-cracking behaviour for the specimens containing the higher transverse reinforcement configurations. The greater deformation sustained by AC5 and AC6 before reaching their maximum load suggests improved post-cracking resistance compared with the beams containing the lower reinforcement levels. However, because only one specimen was tested for each reinforcement configuration, these observations should be interpreted as experimental trends rather than statistically established differences. The investigation clearly suggests that reinforcement detailing, especially stirrup spacing and bar diameter, plays an important role in enhancing the shear performance of HSSCC with manufactured sand.

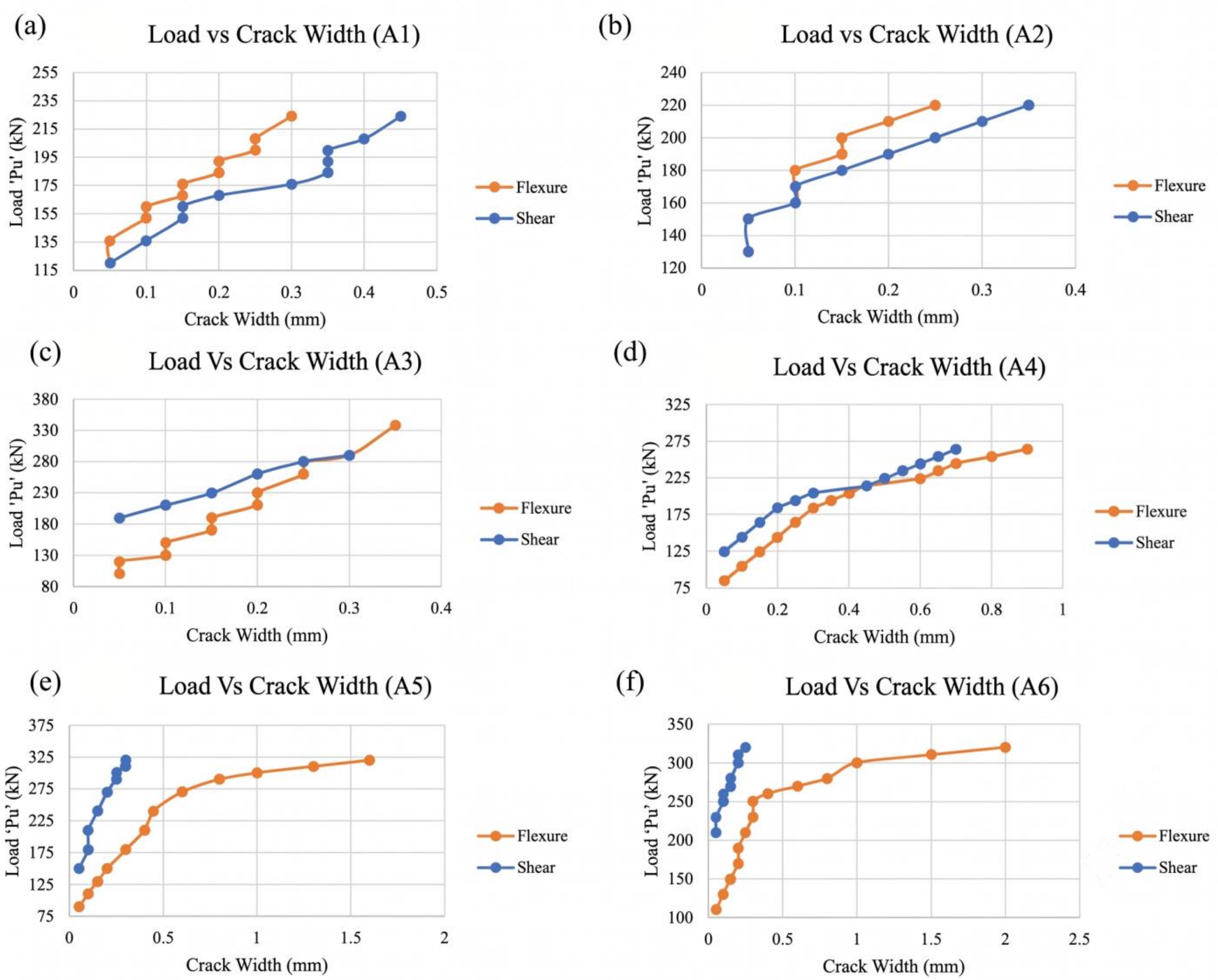

Fig. 2 Load vs crack width for HSSCC AC1-AC6

3.2. Cracking Behaviour

The load–crack-width responses of the six beams are presented in Figure 2. The first visible cracking loads were relatively close for all specimens, ranging from 36 to 44 kN. This limited variation indicates that the initiation of the first visible cracks was not strongly affected by the transverse reinforcement configurations investigated. The relatively similar cracking loads are also consistent with the fact that the concrete mixture, beam geometry and longitudinal reinforcement were maintained constant for all specimens.

Initially, flexural cracks developed in the tension zone, predominantly near the soffit region. With increasing load, these cracks propagated upward. As the applied load increased further, diagonal cracks developed within the shear spans. The subsequent response depended on the reinforcement configuration and the governing failure mechanism.

For the beams exhibiting shear failure, the diagonal cracks progressively extended towards the loading and support regions, followed by rapid widening and loss of shear resistance. In the beams governed by flexural failure, flexural cracking became more pronounced and concrete spalling was observed in the compression zone near the ultimate stage. The change in failure mode with increasing transverse reinforcement indicates that the additional shear reinforcement was effective in delaying or suppressing shear failure, allowing flexural mechanisms to become more critical in some specimens.

The crack-width response also indicates that transverse reinforcement primarily influenced crack propagation after cracking rather than the initiation of the first visible crack. This distinction is important because the initial cracking load is largely associated with the tensile cracking characteristics of the concrete section, whereas the subsequent diagonal crack development is strongly influenced by the interaction between concrete, longitudinal reinforcement and transverse reinforcement.

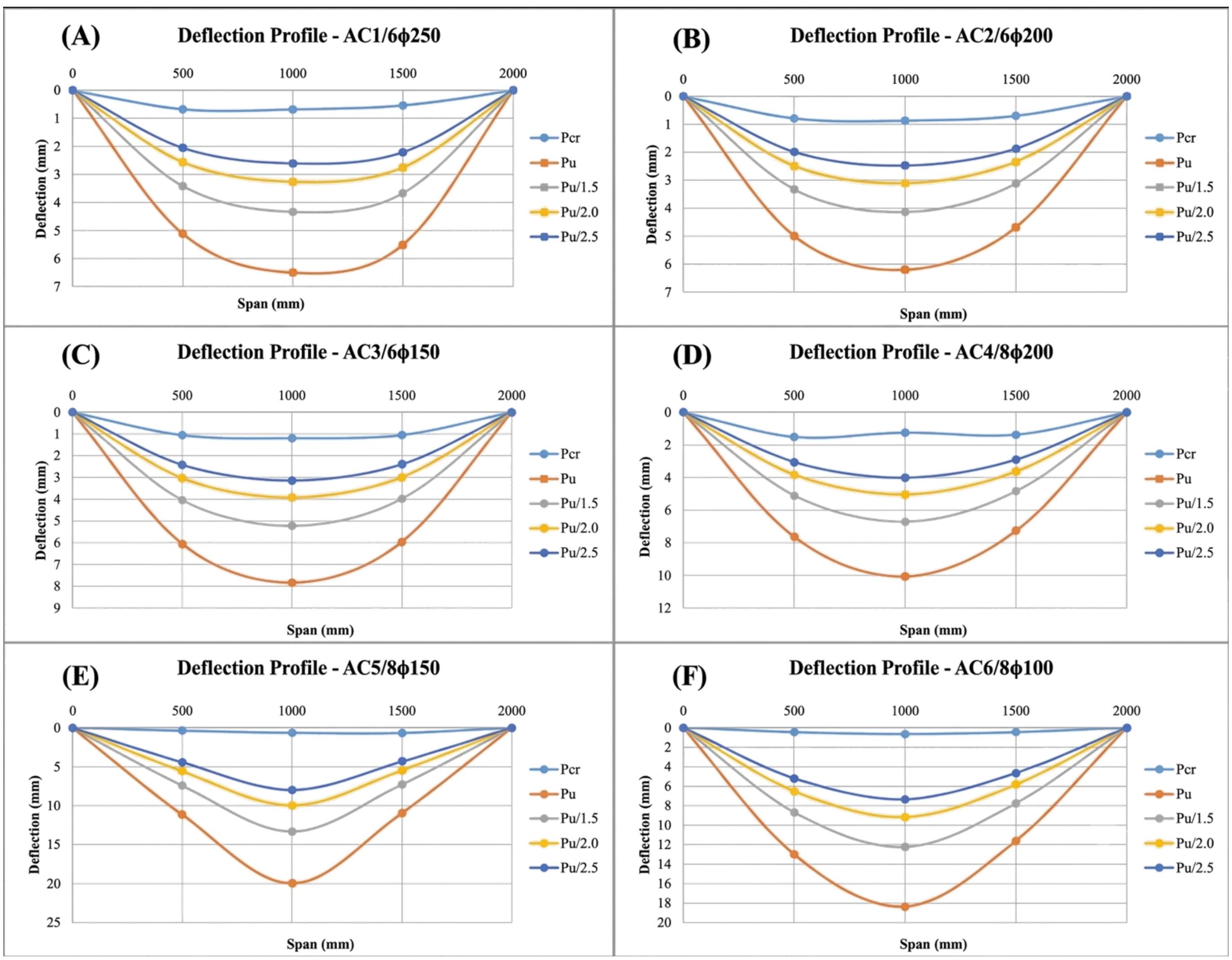

Fig. 3 Deflection profile of HSSCC beams AC1-AC6

3.3. Deflection Response of Beams

The deflection profiles obtained at the one-third-span and two-third-span locations are presented in Figure 3. The profiles were approximately symmetrical about the centre of the beam, as expected for the loading and support arrangement adopted in the experimental programme. At lower load levels, the deflection increased approximately in proportion to the applied load. After cracking, the rate of deformation increased as the stiffness of the cracked section decreased.

The increase in deflection became more pronounced as the specimens approached their ultimate load. The steeper profiles observed at the final loading stage indicate the transition from stable post-cracking behaviour towards the governing failure mechanism. Beams containing greater amounts of transverse reinforcement generally exhibited improved resistance to deformation at comparable loading stages, although the response also depended on the failure mode.

The results, therefore, indicate that transverse reinforcement influences not only the ultimate shear resistance but also the post-cracking deformation behaviour. Nevertheless, the present dataset is insufficient to establish a statistically validated relationship between transverse reinforcement and stiffness or ductility. The observed trends should therefore be regarded as experimental evidence within the investigated reinforcement range.

3.4. Influence of Transverse Reinforcement Ratio on Shear Strength

The relationship between transverse reinforcement ratio ((\rho_w)) and experimental shear strength is presented in Figure 4. The experimental results show an overall increase in shear strength with increasing transverse reinforcement ratio. The measured shear forces increased from 116 kN for AC1 to 169 kN for AC3 within the 6 mm stirrup series. For the 8 mm stirrup series, the corresponding values increased from 154 kN for AC4 to 170 kN for AC5 and remained approximately unchanged for AC6.

The increase from AC1 to AC3 demonstrates the beneficial effect of reducing stirrup spacing when the stirrup diameter is maintained at 6 mm. However, the comparison between AC4, AC5 and AC6 indicates that the relationship is not linear over the complete reinforcement range. Although AC6 contained the highest transverse reinforcement ratio, its experimental shear force was approximately the same as that of AC5. This suggests that, within the range investigated, increasing the reinforcement beyond a certain level did not produce a proportional increase in ultimate shear resistance.

A second-degree polynomial was fitted to the experimental data and produced an (R^2) value of 0.7746. The fitted relationship indicates an overall positive but nonlinear association between transverse reinforcement ratio and experimental shear strength. However, because the relationship is based on only six experimental observations and the reinforcement diameter and spacing were varied simultaneously, it should be interpreted only as an empirical representation of the trend observed in the present study. It should not be considered a generalized predictive equation or used for design outside the investigated range.

The observed trend is consistent with the role of transverse reinforcement in controlling diagonal cracking and contributing tensile resistance across the shear cracks. The limited increase at higher reinforcement levels may be associated with the fact that the ultimate response becomes increasingly governed by other shear-resisting mechanisms and, in some specimens, by flexural behaviour. Therefore, simply increasing transverse reinforcement does not necessarily result in a proportional increase in overall beam capacity.

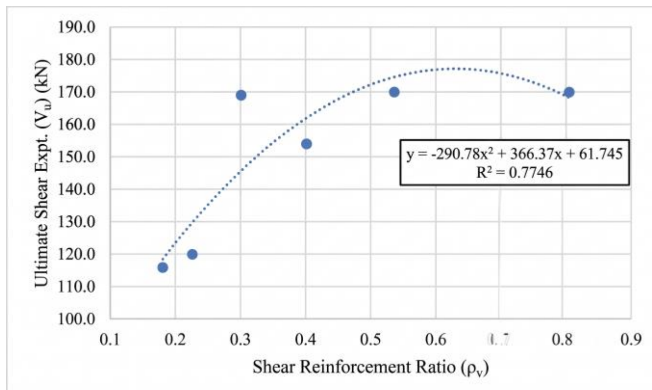

Fig. 4 Correlation between shear reinforcement ratio and experimental shear

3.5. Failure Mode and Effect of Reinforcement Configuration

The experimental failure observations indicate that the governing failure mechanism changed with the amount and configuration of transverse reinforcement. Beams with lower transverse reinforcement were more susceptible to diagonal shear failure, whereas the beams with greater transverse reinforcement showed a greater tendency towards flexural failure.

The observed transition is significant because it demonstrates that increasing transverse reinforcement can shift the critical mechanism from shear towards flexure. This is desirable from a structural safety perspective because flexural failure generally provides greater deformation and warning before collapse than a sudden shear failure. The experimental observations, therefore, support the importance of adequate transverse reinforcement detailing in HSSCC beams.

At the same time, the results indicate that reinforcement diameter and spacing should not be considered independently from the resulting reinforcement ratio. For example, AC5 and AC6 contain the same 8 mm stirrup diameter but different spacings, while their experimental ultimate shear forces were both approximately 170 kN. This indicates that further reduction in spacing beyond the AC5 configuration did not produce a measurable increase in ultimate shear force in the present tests.

3.6. Comparison with Codal and Analytical Predictions

In order to study the behaviour of shear in beams, various codal provisions & design approaches were reviewed along with Response-2000 software and compared. The equations given by different codes and researchers are listed below eq. (1) to eq. (15),

3.6.1. Indian Code of Practice (IS 456:2000)

$$\tau_c = \frac{0.85\sqrt{0.8f_{ck}}(\sqrt{1+5\beta}-1)}{6\beta} \quad (1)$$

$$\beta = \frac{0.8f_{ck}}{6.89\,\rho_t} \geq 1 \quad (2)$$

$$V_{us} = \frac{0.87f_y A_{sv} d}{S_v} \quad (3)$$

$$V_{us} = V_u - \tau_c bd \quad (4)$$

3.6.5. Zsutty's Equation

$$v_u = \begin{cases} 2.1746\left(f_c'\rho\dfrac{d}{a}\right)^{1/3} + \rho_v f_{vy} & for, \quad \left(\dfrac{a}{d}\right) \geq 2.5 \\ 2.5\left(\dfrac{d}{a}\right)\left[2.1746\left(f_c'\rho\dfrac{d}{a}\right)^{1/3}\right] + \rho_v f_y & for, \quad 1.5 < \left(\dfrac{a}{d}\right) < 2.5 \end{cases} \quad (12)$$

3.6.2. Australian Code, AS 3600-2018

$$V_{uc} = \beta_1\beta_2\beta_3 \frac{A_{st}}{b_v d_0}\left(\frac{f_c'}{b_v d_0}\right)^{1/3} b_v d_0 \geq 0.2f_c' b_v d_0 \quad (5)$$

3.6.3. ACI 318-19 [3]

$$V_n = V_c + V_s \quad (6)$$

$$V_c = \left(0.158\sqrt{f_c'} + 17.24\rho_s\frac{V_u d}{M_u}\right) b_w d \quad \leq \quad 0.3\sqrt{f_c'} b_w d \quad (7)$$

$$V_s = \frac{A_v f_{sv} d}{s} > 0.686\sqrt{f_c'} b_w d \quad (8)$$

3.6.4. Japanese Code (JSCE Standards, 2008) [37]

$$V_{yd} = V_{cd} + V_{sd} + V_{ped} \quad (9)$$

$$V_{cd} = 0.9\beta_d\beta_p\beta_n(f_c')^{1/3} \quad (10)$$

For a member without vertical prestressing, $V_{ped} = 0$, and with vertical stirrups, V_{sd} is:

$$V_{sd} = \left(\frac{A_v f_{sv}}{s}\right)\frac{z}{\gamma_b} \quad (11)$$

3.6.6. RILEM TC 162-TDF Approach

$$V_{Rd3} = V_{cd} + V_{fd} + V_{wd} \quad (13)$$

$$V_{fd} = 0$$

$$V_{cd} = \left(0.12k(100\rho_l f_{ck})^{\frac{1}{3}} + 0.15\sigma_{cp}\right) b_w d \quad (14)$$

$$V_{wd} = \frac{A_{sw}}{S}\, 0.9\, d\, f_{ywd}\, (1 + \cot g\alpha)\sin\alpha \quad (15)$$

The experimentally determined shear capacities were compared with the predictions obtained from IS 456:2000, AS 3600:2018, ACI 318-19, JSCE, Zsutty's equation, the RILEM approach and Response-2000. The calculated values and their ratios to the experimental shear capacities are presented in Tables 4 and 5.

The results show that all the considered approaches, with the exception of the AS 3600 prediction for AC6, produced conservative estimates of the experimental shear capacity. The mean ratios of calculated to experimental shear force were 0.411, 0.783, 0.516, 0.401, 0.718, 0.559 and 0.437 for IS 456, AS 3600, ACI 318-19, JSCE, Zsutty, RILEM and Response-2000, respectively.

Among the approaches considered, AS 3600 produced the highest mean (V_{cal}/V_{exp}) ratio of 0.783. Thus, on average, the AS 3600 approach predicted approximately 78% of the experimentally measured shear capacity and underestimated the experimental strength by approximately 21.7%. Although this represents the closest prediction among the methods examined, the result should not be interpreted as exact agreement.

Zsutty's equation provided the second-highest mean ratio of 0.718, corresponding to an average underestimation of approximately 28.2%. The ACI 318-19 and RILEM approaches produced mean ratios of 0.516 and 0.559, respectively, while the IS 456, JSCE and Response-2000 approaches produced lower mean ratios.

These results indicate that the degree of conservatism differs considerably among the prediction approaches for the HSSCC beams investigated.

The coefficient of variation provides an additional measure of consistency. Zsutty produced the lowest coefficient of variation of 14.06%, indicating the smallest scatter among the methods considered, although its mean prediction was substantially lower than the experimental strength. AS 3600 had a coefficient of variation of 23.72%, indicating greater scatter despite producing the highest mean prediction. Zsutty's approach showed a mean ratio of 0.718 with a coefficient of variation of 14.06%. These results demonstrate that accuracy and consistency should be considered separately when evaluating the suitability of a prediction model.

Overall, the comparison indicates that the existing approaches examined in this study generally underestimate the measured shear resistance of the investigated M-sand-based HSSCC beams. This may be associated with differences between the concrete used to develop the original empirical relationships and the HSSCC investigated in the present study, including the high compressive strength, self-compacting characteristics and manufactured-sand aggregate system. However, the present experimental dataset is too limited to establish a modified design equation. The results instead provide an experimental basis for evaluating the conservatism and relative performance of existing approaches for the investigated beam configurations.

3.7. Response – 2000 Analysis [38]

Response-2000 was used to provide an additional analytical assessment of the nonlinear response of the tested beams. Figure 5 presents the predicted response for beam AC6/8ϕ100. The software predicted a nonlinear load–deflection response and provided information on shear capacity and crack development. For AC6, the Response-2000 analysis reported an ultimate shear capacity of 64.8 kN at a deflection of approximately 5.3 mm, whereas the experimental shear force was 170 kN. The predicted-to-experimental ratio was therefore approximately 0.381. The predicted result is substantially lower than the experimental capacity, indicating that the software was conservative for this specimen.

The Response-2000 crack pattern showed distributed cracking along the member, with greater crack widths in regions associated with high moment and shear. This qualitative feature is consistent with the experimentally observed development of flexural and shear cracks. However, the substantial difference between predicted and experimental shear capacity indicates that the analytical model did not reproduce the full shear resistance observed in the tested M-sand-based HSSCC beam.

It should be noted that the compressive strength values used in the experimental and analytical investigations are expressed on different specimen bases. For beam AC6, the experimentally determined compressive strength was 74.86 MPa based on cube specimens, whereas the compressive strength adopted as input in the Response-2000 analysis was 59.9 MPa, expressed in terms of cylindrical compressive strength. The value of 59.9 MPa was therefore used as the concrete compressive strength parameter in the Response-2000 model to maintain consistency with the cylindrical-strength basis of the analytical input.

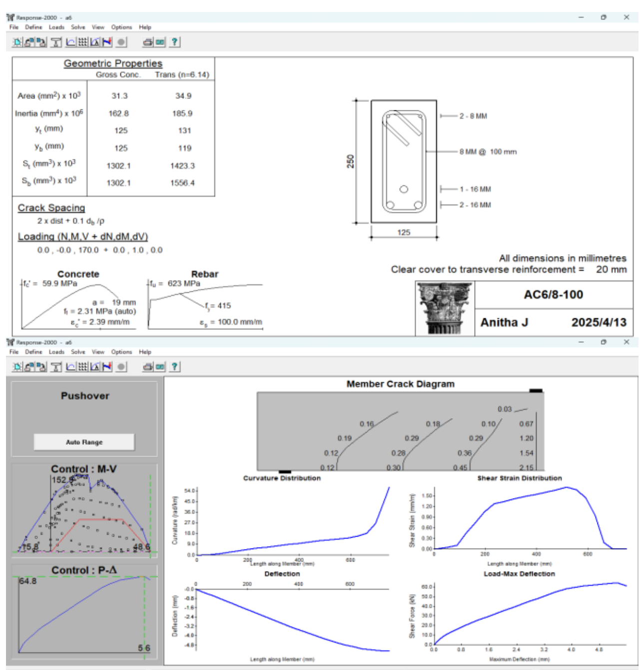

Fig. 5 Member response from Response-2000

Table 4. Ratio of computed shear force to ultimate shear force ratio

Beam Designation	Expt. Ultimate Shear (kN)	Vu calculated/ Vu experimental						
		IS 456	AS 3600	ACI 318	JSCE 86	Zsutty	RILEM	Response-2000
AC1/6ϕ250	116	0.360	0.673	0.468	0.368	0.722	0.474	0.529
AC2/6ϕ200	120	0.383	0.721	0.494	0.387	0.741	0.510	0.530
AC3/6ϕ150	169	0.311	0.585	0.391	0.306	0.563	0.416	0.382
AC4/8ϕ200	154	0.401	0.764	0.500	0.389	0.692	0.546	0.418
AC5/8ϕ150	170	0.435	0.835	0.537	0.416	0.711	0.600	0.379
AC6/8ϕ100	170	0.577	1.121	0.703	0.541	0.878	0.810	0.381
Mean		0.411	0.783	0.516	0.401	0.718	0.559	0.437
SD		0.09	0.19	0.10	0.08	0.10	0.14	0.07
CV		22.23	23.72	20.18	19.39	14.06	24.60	16.82
Mean Error (%)		-58.9	-21.7	-48.5	-59.9	-28.2	-44.1	-56.3

Table 5. Computed shear and ultimate shear

Beam Designation	Vu expt (kN)	Computed Shear (kN)						
		IS 456	AS 3600	ACI 318	JSCE 86	Zsutty	RILEM	Response-2000
AC1/6ϕ250	116	41.79	78.05	54.29	42.73	83.79	55.00	61.4
AC2/6ϕ200	120	45.94	86.51	59.32	46.49	88.95	61.20	63.6
AC3/6ϕ150	169	52.52	98.92	66.02	51.69	95.16	70.38	64.6
AC4/8ϕ200	154	61.72	117.62	77.07	59.97	106.49	84.09	64.3
AC5/8ϕ150	170	73.88	142.00	91.27	70.67	120.82	101.99	64.5
AC6/8ϕ100	170	98.16	190.61	119.51	91.97	149.25	137.69	64.8

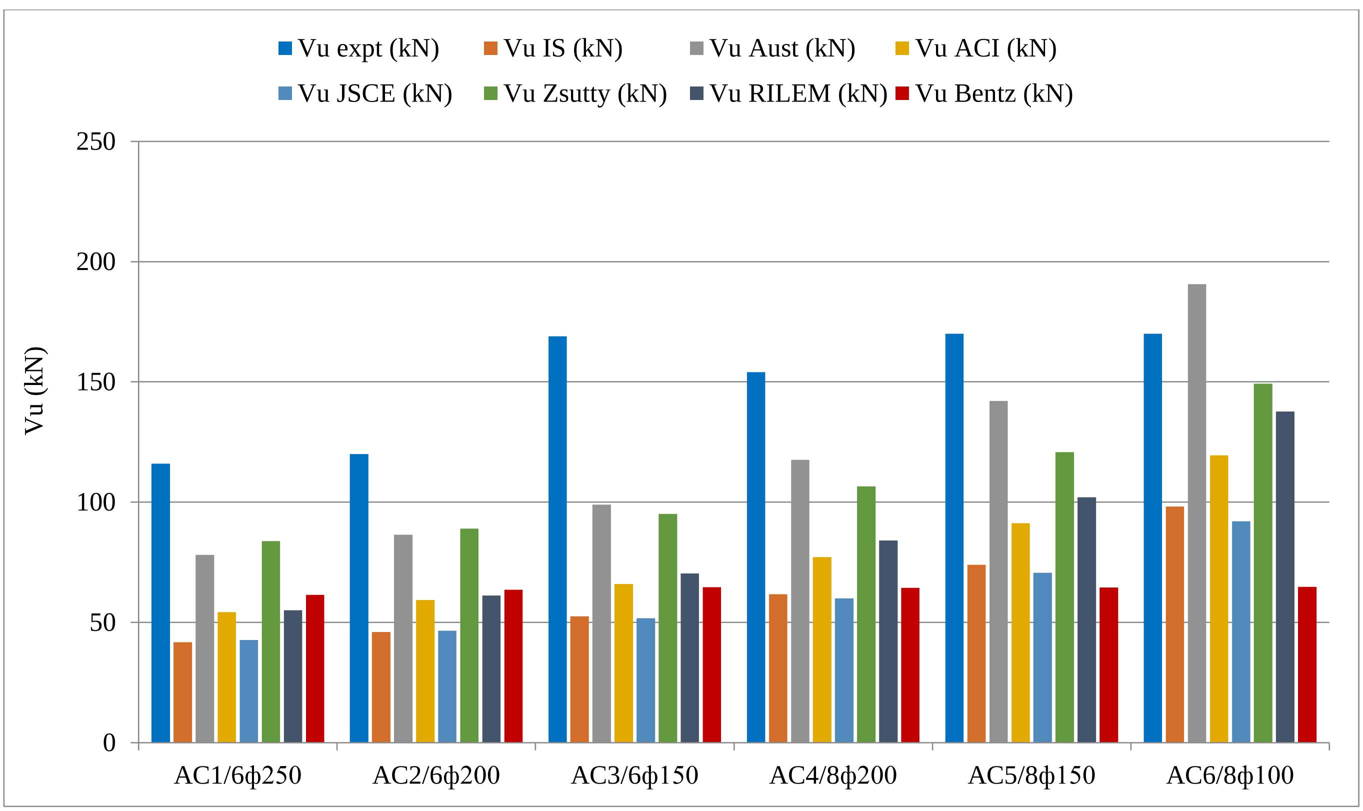

Fig. 6 Comparison of shear forces

The comparatively better performance of AS 3600 may be associated with the formulation adopted for shear resistance, which considers the concrete contribution and transverse-reinforcement contribution together and incorporates parameters related to effective depth, transverse reinforcement and the variable concrete contribution factor (k_v). Such features are relevant to the present experimental programme because the principal variable among the specimens was the amount and configuration of transverse reinforcement. The AS 3600 formulation also incorporates a variable compression-strut angle, providing a mechanism-based treatment of the contribution of shear reinforcement. These characteristics may have contributed to its comparatively closer prediction of the experimentally measured shear capacities.

The substantial underestimation obtained from several approaches may be related to differences between the material and structural characteristics of the present specimens and the experimental databases or assumptions underlying the respective formulations. The present beams were produced using M70 high-strength self-compacting concrete with manufactured sand and contained relatively high-strength concrete and varying transverse reinforcement. Contributions from aggregate interlock, dowel action of longitudinal reinforcement and the interaction between concrete and transverse reinforcement may therefore differ from those implicitly represented in the empirical formulations.

The present comparison should nevertheless be interpreted within the limits of the six experimental specimens. The results demonstrate the relative performance of the selected prediction approaches for the particular M-sand-based HSSCC beam configurations investigated, but they do not establish the universal superiority of AS 3600 or justify modification of any existing design equation. A larger experimental database covering different concrete strengths, beam sizes, shear-span-to-depth ratios and reinforcement configurations would be required before a generalized predictive relationship could be proposed.

3.8. Overall Discussion of Experimental Findings

The experimental results demonstrate that transverse reinforcement has a clear influence on the shear response of M-sand-based HSSCC beams. Increasing transverse reinforcement generally improved ultimate shear resistance and delayed the development of critical diagonal cracking. The effect was particularly evident within the 6 mm stirrup series, where reducing spacing from 250 to 150 mm increased experimental shear force from 116 to 169 kN.

However, the results also demonstrate that the relationship between transverse reinforcement and shear capacity is not unlimited or linear. The 8 mm stirrup series showed an increase from 154 kN for AC4 to approximately 170 kN for AC5, while a further increase in reinforcement ratio in AC6 did not increase the experimental shear force. This behaviour suggests that other shear-resisting mechanisms become increasingly important at higher transverse reinforcement levels.

The relatively similar first-cracking loads, combined with the substantial differences in ultimate shear capacity, further indicate that transverse reinforcement has a greater influence on the post-cracking and ultimate response than on the initiation of the first visible crack. This distinction is important when interpreting the role of stirrups in HSSCC beams.

The comparison with existing prediction methods indicates that the tested beams developed greater shear resistance than predicted by most of the evaluated approaches. AS 3600 provided the highest average prediction relative to the experimental results, while RILEM provided the lowest scatter. Nevertheless, none of the investigated approaches reproduced the complete experimental response with sufficient accuracy to justify adoption as a specific predictive model for M-sand-based HSSCC based solely on the present six-beam dataset.

The results therefore support the need for further experimental investigation involving a broader range of concrete strengths, beam sizes, shear-span-to-effective-depth ratios, aggregate characteristics and transverse reinforcement ratios. Such an expanded database would be required before developing or calibrating a generalized shear-strength expression specifically for M-sand-based HSSCC.

4. Conclusion

Based on the experimental investigation of six reinforced M70 high-strength self-compacting concrete beams incorporating manufactured sand and different transverse reinforcement configurations, the following conclusions are drawn:

1. The experimental results demonstrate that transverse reinforcement has a significant influence on the shear response of M-sand-based HSSCC beams. Increasing the amount of transverse reinforcement generally increased the ultimate shear resistance and delayed the development of critical diagonal cracking.
2. Within the 6 mm stirrup series, reducing the stirrup spacing from 250 mm in AC1 to 150 mm in AC3 increased the experimental shear force from 116 kN to 169 kN, corresponding to an increase of approximately 45.7%. This confirms the beneficial contribution of closer transverse reinforcement to the shear resistance of HSSCC beams.
3. The 8 mm stirrup series showed a similar but non-linear trend. The experimental shear force increased from 154 kN for AC4 to 170 kN for AC5, whereas a further increase in transverse reinforcement in AC6 did not produce an additional increase in the measured ultimate shear force. This indicates that the increase in shear

capacity was not proportional to the increase in transverse reinforcement over the complete range investigated.

4. The first visible cracking loads of the six beams were relatively similar, ranging from 36 to 44 kN. This indicates that the variation in transverse reinforcement had a comparatively limited influence on the initiation of the first visible cracks, while its influence became more pronounced during subsequent crack propagation and the ultimate loading stage.
5. The observed failure behaviour indicates a transition in the governing response with changes in transverse reinforcement. Beams with lower transverse reinforcement were more susceptible to shear-controlled behaviour, whereas higher transverse reinforcement configurations exhibited greater resistance to diagonal cracking and, in some specimens, a shift towards flexural behaviour. This demonstrates the importance of adequate transverse reinforcement in reducing the likelihood of brittle shear failure.
6. An overall positive relationship was observed between the transverse reinforcement ratio ((ρ_w)) and experimental shear strength. The second-degree polynomial fitted to the six experimental observations produced an (R^2) value of 0.7746. However, this relationship represents only the trend observed within the investigated experimental range and should not be considered a generalized predictive or design equation because of the limited number of specimens.
7. Comparison with existing codal and analytical approaches showed that most of the evaluated methods underestimated the experimentally measured shear capacity. The mean (V_{cal}/V_{exp}) ratios were 0.411, 0.783, 0.516, 0.401, 0.718, 0.437 and 0.559 for IS 456, AS 3600, ACI 318-19, JSCE, Zsutty, RILEM and Response-2000, respectively.
8. Among the evaluated approaches, AS 3600 provided the closest mean prediction, with an average (V_{cal}/V_{exp}) ratio of 0.783, corresponding to an average underestimation of approximately 21.7%. However, AS 3600 overestimated the capacity of AC6 by approximately 12.1%. Therefore, the results demonstrate comparatively better agreement of AS 3600 for the present experimental dataset, but do not establish its universal superiority for HSSCC beams.
9. Zsutty's equation provided the second-closest mean prediction, with a (V_{cal}/V_{exp}) ratio of 0.718 and an average underestimation of approximately 28.2%. In terms of prediction scatter, Zsutty's equation produced the lowest coefficient of variation among the evaluated approaches, whereas AS 3600 provided the closest mean prediction.
10. The Response-2000 analysis of AC6 predicted an ultimate shear capacity of 64.8 kN compared with the experimental value of 170 kN. Although the analytical model reproduced the general nonlinear nature of the beam response and distributed cracking behaviour, it substantially underestimated the experimentally observed shear capacity for this specimen.
11. Overall, the experimental findings demonstrate that M70 HSSCC incorporating manufactured sand can develop substantial shear resistance when adequate transverse reinforcement is provided. The results also indicate that the interaction between concrete strength, manufactured-sand aggregate characteristics, longitudinal reinforcement and transverse reinforcement contributes to the observed shear response and should be considered when assessing the applicability of existing shear-strength prediction approaches.
12. The findings are limited to the six beam configurations, M70 HSSCC mixture, beam dimensions and reinforcement ranges investigated in the present study. Further experimental studies involving additional beam sizes, concrete strengths, shear-span-to-effective-depth ratios, manufactured-sand characteristics and transverse reinforcement levels are required to establish a broader database and to develop or validate generalized shear-strength prediction models for M-sand-based HSSCC.

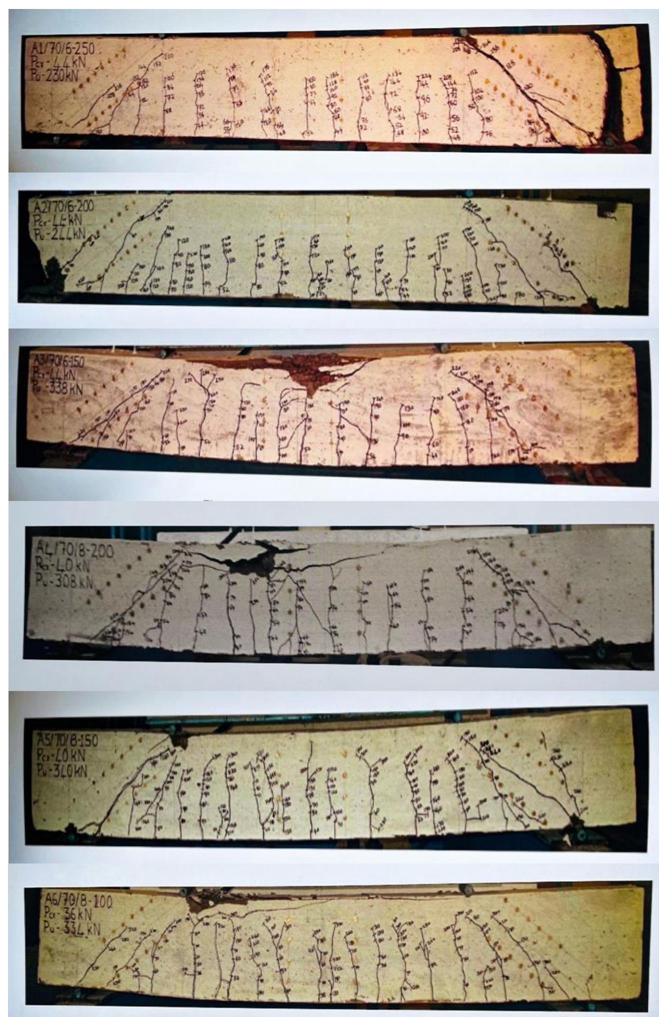

Fig. 7 Crack pattern of HSSCC beams AC1-AC6

Notations

b, b_v, b_w = width of beam
d, d_o = effective depth of beam
l = effective span
a = shear span
τ_C = design shear stress of concrete
β = reinforcement index
A_{st} = area of longitudinal steel
$\beta_1 = 1.1\left(1.6 - \frac{d_o}{1000}\right) \geq 1.1$
β_2 = 1 (Where no axial load exists)
$= 1 - \frac{N}{3.5A_g}$; Subjected to axial tension
$= 1 - \frac{N}{14A_g}$; Subjected to axial compression

$\beta_3 = 2\frac{d_o}{a} \leq 2$; Concentrated load
= 1/4; Uniformly Distributed Load

f_y, f_{ywd}, f_{vy} = Yield strength of the shear reinforcement
A_{sv}, A_v = Area of shear reinforcement
f_{sv} = Yield strength of stirrup reinforcement
s, s_v = Spacing of the stirrups
f_{ck} = Characteristic Compressive strength of concrete

$\beta_d = \left(\frac{100}{d}\right)^{1/4} \leq 1.5,\ d\ is\ in\ cm$

$\beta_p = (100\rho)^{1/3} \leq 1.5$

$\beta_n = 1 + \frac{M_0}{M_d} \leq 2.0\ (N_d' \geq 0)$

$= 1 + \frac{2M_0}{M_d} \geq 0\ (N_d' < 0)$

$= 1.0\ (as\ M_0 = 0)$

M_a = design flexural moment
M_0 = decompression moment that causes an extreme bottom fiber stress of zero when combined with the axial stress.
ρ_v, ρ_w = Shear reinforcement ratio
ρ, ρ_l = Tensile reinforcement ratio
fy = Characteristic strength of tensile steel
f_c' = Characteristic Cylindrical Compressive strength of concrete
N_{sd} = axial force due to applied load,
A_{sw} = Cross section area of the arms of the stirrups

Conflicts of Interest

The authors declare that there is no conflict of interest regarding the publication of this paper.

Funding Statement

No funding received from any sources.

References

[1] *ACI Building Code Requirements for Reinforced Concrete (ACI 318-63)*, Detroit, MI, USA: American Concrete Institute, 1963. [Google Scholar] [Publisher Link]

[2] *Building Code Requirements for Structural Concrete (ACI 318-14) and Commentary (ACI 318R-14)*, Farmington Hills, MI, USA: American Concrete Institute, 2014. [Google Scholar] [Publisher Link]

[3] *Building Code Requirements for Structural Concrete (ACI 318-19)*, Farmington Hills, MI, USA: American Concrete Institute, 2019. [Publisher Link]

[4] Gaetano Russo, Giuliana Somma, and Denis Mitri, "Shear Strength Analysis and Prediction for Reinforced Concrete Beams without Stirrups," *Journal of Structural Engineering*, vol. 131, no. 1, pp. 66-74, 2005. [CrossRef] [Google Scholar] [Publisher Link]

[5] Hong-Gun Park et al., "Shear Strength of Simply- or Rigidly-Supported RC Beams with Various Design Variables," *Advances in Structural Engineering*, vol. 15, no. 12, pp. 2071-2084, 2012. [CrossRef] [Google Scholar] [Publisher Link]

[6] M. Hamrat et al., "Shear Behaviour of RC Beams without Stirrups Made of Normal Strength and High Strength Concretes," *Advances in Structural Engineering*, vol. 13, no. 1, pp. 29-41, 2010. [CrossRef] [Google Scholar] [Publisher Link]

[7] Güray Arslan, "Shear Strength of Reinforced Concrete Beams with Stirrups," *Materials and Structures*, vol. 41, pp. 113-122, 2008. [CrossRef] [Google Scholar] [Publisher Link]

[8] Sang-Woo Kim, "Prediction of Shear Strength of Reinforced High-Strength Concrete Beams using Compatibility-Aided Truss Model," *Applied Sciences*, vol. 11, no. 22, pp. 1-12, 2021. [CrossRef] [Google Scholar] [Publisher Link]

[9] G. Russo, G. Somma, and P. Angeli, "Design Shear Strength Formula for High Strength Concrete Beams," *Materials and Structures*, vol. 37, no. 10, pp. 680-688, 2004. [CrossRef] [Google Scholar] [Publisher Link]

[10] G.N.J. Kani, "Basic Facts Concerning Shear Failure," *ACI Proceedings*, vol. 63, no. 6, pp. 675-692, 1966. [CrossRef] [Google Scholar] [Publisher Link]

[11] K. S. Rajagopalan, and Phil M. Ferguson, "Exploratory Shear Tests Emphasizing Percentage of Longitudinal Steel," *ACI Proceedings*, vol. 65, no. 8, pp. 634-638, 1968. [CrossRef] [Google Scholar] [Publisher Link]

[12] *Building Code Requirements for Reinforced Concrete (ACI 318-83)*. Farmington Hills, MI, USA: American Concrete Institute, 1983. [Google Scholar] [Publisher Link]

[13] Roger Diaz De Cossio, and Chester P. Siess, "Behavior and Strength in Shear of Beams and Frames without Web Reinforcement," *ACI Proceedings*, vol. 56, no. 8, pp. 695-731, 1960. [CrossRef] [Google Scholar] [Publisher Link]

[14] Robert G. Mathey, and David Watstein, "Shear Strength of Beams without Web Reinforcement Containing Deformed Bars of Different Yield Strengths," *ACI Structural Journal*, vol. 60, no. 2, pp. 183-208, 1963. [CrossRef] [Google Scholar] [Publisher Link]

[15] Boris Bresler, and A. C. Scordelis, "Shear Strength of Reinforced Concrete Beams," *ACI Structural Journal*, vol. 60, no. 1, pp. 51-74, 1963. [CrossRef] [Google Scholar] [Publisher Link]

[16] William J. Krefeld, and Charles W. Thurston, "Studies of the Shear and Diagonal Tension Strength of Simply Supported Reinforced Concrete Beams," *ACI Proceedings*, vol. 63, no. 4, pp. 451-476, 1966. [CrossRef] [Google Scholar] [Publisher Link]

[17] Theodore Zsutty, "Shear Strength Prediction for Separate Categories of Simple Beam Tests," *ACI Structural Journal*, vol. 68, no. 2, pp. 138-143, 1971. [CrossRef] [Google Scholar] [Publisher Link]

[18] Alan H. Mattock, and Zuhua Wang "Shear Strength of Reinforced Concrete Members Subject to High Axial Compressive Stress," *ACI Structural Journal*, vol. 81, no. 3, pp. 287-298, 1984. [CrossRef] [Google Scholar] [Publisher Link]

[19] *Building Code Requirements for Reinforced Concrete (ACI 318-77)*, Detroit, MI, USA: American Concrete Institute, 1977. [Google Scholar] [Publisher Link]

[20] *426.1R-77 Suggested Revisions to Shear Provisions for Building Codes*, Detroit, MI, USA: American Concrete Institute, 1979. [Google Scholar] [Publisher Link]

[21] Zdenek P. Bazant, and Jin-Keun Kim, "Size Effect in Shear Failure of Longitudinally Reinforced Beams," *ACI Structural Journal*, vol. 81, no. 5, pp. 456-468, 1984. [CrossRef] [Google Scholar] [Publisher Link]

[22] Zdenek P. Bazant, and Hsu-Huei Sun, "Size Effect in Diagonal Shear Failure: Influence of Aggregate Size and Stirrups," *ACI Structural Journal*, vol. 84, no. 4, pp. 259-272, 1987. [CrossRef] [Google Scholar] [Publisher Link]

[23] John J. Roller, and Henry G. Russel, "Shear Strength of High-Strength Concrete Beams with Web Reinforcement," *ACI Structural Journal*, vol. 87, no. 2, pp. 191-198, 1990. [CrossRef] [Google Scholar] [Publisher Link]

[24] Kim Jin-Keun, and Park Yon-Dong, "Shear Strength of Reinforced High Strength Concrete Beams Without Web Reinforcement," *Magazine of Concrete Research*, vol. 46, no. 166, pp. 7-16, 1994. [CrossRef] [Google Scholar] [Publisher Link]

[25] *CEB-FIP Model Code 1990*, Liaison Committee of International Associations - CEB-ACI, 1991. [Google Scholar] [Publisher Link]

[26] Shuaib H. Ahamad, Yuliang Xie, and Tiejun Yu, "Shear Strength of Reinforced Lightweight Concrete Beams of Normal and High Strength Concrete," *Magazine of Concrete Research*, vol. 46, no. 166, pp. 57-66, 1994. [CrossRef] [Google Scholar] [Publisher Link]

[27] Fumio Watanabe, and Jung-Yoon Lee, "Theoretical Prediction of Shear Strength and Failure Mode of Reinforced Concrete Beams," *ACI Structural Journal*, vol. 95, no. 6, pp. 749-757, 1998. [CrossRef] [Google Scholar] [Publisher Link]

[28] Young-Soo Yoon, William D. Cook, and Denis Mitchell, "Minimum Shear Reinforcement in Normal, Medium, and High-Strength Concrete Beams," *ACI Structural Journal*, vol. 93, no. 5, pp. 576-584, 1996. [CrossRef] [Google Scholar] [Publisher Link]

[29] *Design of Concrete Structures*, Canadian Standards Association, CSA A23.3-94, Rexdale, ON, Canada, 1994. [Publisher Link]

[30] Dino Angelakos, Evan C. Bentz, and Michael P. Collins, "Effect of Concrete Strength and Minimum Stirrups on Shear Strength of Large Members," *ACI Structural Journal*, vol. 98, no. 3, pp. 291-300, 2001. [CrossRef] [Google Scholar] [Publisher Link]

[31] A. Cladera, and A.R. Marí, "Shear Design Procedure for Reinforced Normal and High-Strength Concrete Beams Using Artificial Neural Networks. Part II: Beams with Stirrups," *Engineering Structures*, vol. 26, no. 7, pp. 927-936, 2004. [CrossRef] [Google Scholar] [Publisher Link]

[32] A. Cladera, and A. R. Mari, "Shear Design Procedure for Reinforced and Prestressed High- and Normal-Strength Concrete Beams," *ACI Structural Journal*, vol. 228, no. 4, pp. 651-668, 2005. [CrossRef] [Google Scholar] [Publisher Link]

[33] E.C. Bentz, "Empirical Modelling of Reinforced Concrete Shear Strength Size Effect for Members without Stirrups," *ACI Structural Journal*, vol. 102, no. 2, pp. 232-241, 2005. [CrossRef] [Google Scholar] [Publisher Link]

[34] Jung-Yoon Lee et al., "Shear Behavior and Diagonal Crack Width for Reinforced Concrete Beams with High-Strength Shear Reinforcement," *ACI Structural Journal*, vol. 112, no. 3, pp. 323-334, 2015. [CrossRef] [Google Scholar] [Publisher Link]

[35] Walid Mansour, and Bassam A. Tayeh, "Shear Behaviour of RC Beams Strengthened by Various Ultrahigh Performance Fibre-Reinforced Concrete Systems," *Advances in Civil Engineering*, vol. 2020, no. 1, pp. 1-18, 2020. [CrossRef] [Google Scholar] [Publisher Link]

[36] K. Söğüt, "Shear Behaviour of RC Beams: A Numerical Study," *International Journal of Computational and Experimental Science and Engineering*, vol. 9, no. 3, pp. 248-252, 2023. [CrossRef] [Google Scholar] [Publisher Link]

[37] Standard Specifications for Concrete Structures—Design (JSCE Guidelines for Concrete), Japan Society of Civil Engineers, pp. 1-503, 2008, [Online]. Available: https://www.jsce-int.org/system/files/JGC15_Standard_Specifications_Design_1.0.pdf

[38] Evan C. Bentz, *Sectional Analysis of Reinforced Concrete Members*, Response-2000, University of Toronto, pp. 1-86, 2000. [Publisher Link]

[39] Aijaz Ahmad Zende, R.B. Khadiranaikar, and Asif Iqbal. A. Momin, "Shear Behaviour of High Strength Self-Compacting Concrete with Varying Stirrup Spacing," *International Journal of Structural Engineering*, vol. 12, no. 4, pp. 374-387, 2022. [CrossRef] [Google Scholar] [Publisher Link]

[40] Murali Sagar Varma Sagi, Chandrashekhar Lakavath, and S. Suriya Prakash, "Effect of Steel Fibers on the Shear Behavior of Self-Compacting Reinforced Concrete Deep Beams: An Experimental Investigation and Analytical Model," *Engineering Structures*, vol. 269, 2022. [CrossRef] [Google Scholar] [Publisher Link]

[41] Gustavo Savaris, and Isabela de Gois Laufer, "Shear Strength of Steel Fiber Self-Compacting Concrete Beams," *Seminar on Exact and Technological Sciences*, vol. 42, no. 1, pp. 45-62, 2021. [CrossRef] [Google Scholar] [Publisher Link]

[42] S.S. Alkhattat, and M.A. Al-Ramahee, "Shear Performance of Reinforced Self-Compacting Concrete Beams Incorporating Steel and Polypropylene Fibers," *Scientific Review Engineering and Environmental Sciences*, vol. 30, no. 4, pp. 537-551, 2022. [CrossRef] [Google Scholar] [Publisher Link]

[43] Isabela Ereno da Silva et al., "Shear Strength of Hybrid Fiber Reinforced Self-Compacting Concrete Beams," *Semina: Exact and Technological Sciences*, vol. 44, pp. 1-11, 2023. [CrossRef] [Google Scholar] [Publisher Link]

[44] Ahmed Awad et al., "Effect of Hybrid-Fiber-Reinforcement on the Shear Behavior of High-Strength-Concrete Beams," *Frontiers in Materials*, vol. 9, pp. 1-18, 2023. [CrossRef] [Google Scholar] [Publisher Link]

[45] Husain Abbas et al., "Shear Strength of Functionally Graded Self-Compacting Concrete Deep Beams Reinforced with Steel and GFRP Bars," *Case Studies in Construction Materials*, vol. 18, pp. 1-19, 2023. [CrossRef] [Google Scholar] [Publisher Link]

[46] Jin-Seok Choi et al., "Shear Strengthening of Self-Compacting Lightweight Concrete Beams with Steel Fibers and Unbonded Prestressing Bars," *Engineering Structures*, vol. 317, 2024. [CrossRef] [Google Scholar] [Publisher Link]

[47] Cahya Erwanto et al., "Shear Behavior of High-Volume Fly Ash Self-Compacting Concrete (HVFA-SCC) T-Beams Strengthened with Carbon Fiber Reinforced Polymer (CFRP)," *E3S Web of Conferences*, vol. 725, pp. 1-12, 2026. [CrossRef] [Google Scholar] [Publisher Link]

[48] Yaojia Chen et al., "Shear Performance and Fracture Behavior in Reinforced Manufactured Sand-Based Ultra-High Performance Concrete Beams: Experimental Investigation, Damage Characterization, and Theoretical Analysis," *Engineering Fracture Mechanics*, vol. 332, 2026. [CrossRef] [Google Scholar] [Publisher Link]